P1.7 CLOUD OPTICAL AND MICROPHYSICAL PROPERTIES DERIVED FROM SATELLITE DATA

Cristian Mitrescu[1,2,*] Steve Miller[2] Robert Wade[3]

[1]American Society for Engineering Education
[2]Naval Research Laboratory, Marine Meteorology Division, Monterey, California
[3]Science Applications International Corporation, Monterey, California

1. INTRODUCTION

It is now well established that the complex nonlinear interactions and feedbacks generated by clouds modulate the climate response on many spatial and temporal scales (Liou, 1986; Ramanathan and Collins, 1991; Held and Soden, 2000; Hartmann and Larson, 2002; etc.). To better assess these processes, the global distribution of both large- and small-scale cloud systems must be measured and their properties quantified in great detail. Data collected by the existing multitude of satellite-based remote sensors are ideal in addressing this task. The use of multi-spectral information is motivated by the aforementioned complex nature of clouds, thus the ability of the forward model to properly describe the observing vector in terms of the relevant state vector (here, cloud microphysical properties) components. The task of retrieving the cloud properties state vector is complicated by the fact that the majority of the sensors are passive and therefore biased toward cloud top. As such, cloud vertical structure is usually neglected altogether (or else assumed crudely) in the forward model.

Present work focuses on the retrieval problem itself, by seeking more accurate and faster algorithms to deal with nonlinearities of forward models. In preparation for the next generation of sensors on board the National Polar-orbiting Operational Environmental Satellite System (NPOESS), the retrieval algorithms - formulated here in terms of the optimal estimation framework, are tested on the Geostationary Operational Environmental Satellites (GOES), using a 3 channel observing system. The retrieved cloud variables of interest are cloud top temperature, cloud top effective radius and cloud optical depth, from which liquid water path, emissivity, and cloud top height are derived. These parameters bear relevance on other topics of interest for Navy applications, such as drizzling marine stratocumulus or convective clouds, for which the observing system must be extended beyond NPOESS capabilities. Currently, daytime retrievals demonstrate the feasibility of the problem, while nighttime retrievals are not as promising due to less sensitivity of the forward model description to the state vector components.

* *Corresponding author address*: Cristian Mitrescu, Naval Research Laboratory, 7 Grace Hopper Ave. MS#2, Monterey, CA 93943-5502; e-mail:cristian.mitrescu@nrlmry.navy.mil

2. OPTIMAL ESTIMATION FRAMEWORK

The principle of remote sensing of a target is based on measuring its emitted and/or scatter radiation. In most cases, this is a complicated function of the state of the system being sensed. *Estimation* (or *filtering*) is the problem of determining such a state from noisy measurements. A key aspect in solving this problem is the specification of a physical model that relates the measurements to the state variables, referred to as the *forward model*. Expressed in a general way, the most probable state of a system given the measurements minimizes the cost function (Jazwinski, 1970; Mitrescu et al., 2005):

$$J(\mathbf{x}) = \tfrac{1}{2}\ [\mathbf{y} - \mathbf{H}(\mathbf{x},\mathbf{b})]^T\ \mathbf{R}^{-1}\ [\mathbf{y} - \mathbf{H}(\mathbf{x},\mathbf{b})] \qquad (1)$$

H is the (nonlinear) forward model describing it in terms of state vector **x** and model parameters **b**. **R** is the error covariance matrix associated with the measurements. We define one component of the state vector by x_k, where k identifies the physical variable. From an initial guess $\mathbf{x}_0$, a better solution to our problem is a state vector that is corrected by an elementary step $\Delta\mathbf{x}$ given by:

$$\Delta\mathbf{x} = \mathbf{S}^{-1}\ (\partial\mathbf{H}/\partial\mathbf{x})^T\ \mathbf{R}^{-1}\ [\mathbf{y} - \mathbf{H}(\mathbf{x},\mathbf{b})] \qquad (2)$$

where

$$\mathbf{S} = (\partial\mathbf{H}/\partial\mathbf{x})^T\ \mathbf{R}^{-1}\ (\partial\mathbf{H}/\partial\mathbf{x}) \qquad (3)$$

is the error covariance matrix of the state vector. Its diagonal elements are variances of the state vector and give a measure of the uncertainty in the retrieval; off-diagonal elements are cross-correlations of the errors. When estimating total error, the observation error covariance matrix **R** contains both measurement errors as well as errors due to uncertainty in forward model parameters **b**:

$$\mathbf{S} = \mathbf{Y} + (\partial\mathbf{H}/\partial\mathbf{b})^T\ \mathbf{R}^{-1}\ (\partial\mathbf{H}/\partial\mathbf{b}) \qquad (4)$$

Here **B** is the model parameter error covariance matrix and **Y** is the measurement error covariance matrix.

3. RADIATIVE TRANSFER MODEL

Following previous work in the field (e.g. Nakajima and King, 1990; Miller et al., 2000; Heidinger, 2003; etc.) a physical model that relates key microphysical and thermodynamical parameters (i.e. the state vector) to the satellite radiometer measurements (i.e. the observing vector) must be formulated. Given the complexity of clouds (in particular ice clouds, due to complex crystal morphology), only general (i.e. statistically relevant) cloud properties may be retrieved. Thus, the forward model must be formulated in such a way that it is complicated enough to capture essential cloud radiative characteristics, yet simple enough for the inversion procedure. Since data from a multi-spectral observing system is to be used, each channel must be explicitly accounted for. For our application, we use GOES channels 1, 2 and 4 for daytime retrievals, and channels 2, 4 and 5 for nighttime retrievals. In each case, the spectral response function of each channel is taken into account. The radiative properties of a clear-sky atmosphere were pre-computed using the **modtran3.5-v1.1** radiative transfer package.

The retrieved state vector quantities are cloud optical depth (defined at ch1 frequency), cloud top effective radius, and cloud top temperature.

3.1 Microphysical model

Following the work of Mitrescu et al., 2005 we assume that cloud particles follow a Gamma size distribution, defined by a characteristic diameter D_0 and a width parameter ν - set to two in the present application, valid for the entire cloud column (i.e. homogeneous cloud):

$$n(D) = N_0 \, 1/\Gamma(\nu) \, (D/D_0)^{\nu-1} \, 1/D_0 \exp(-D/D_0) \qquad (5)$$

Then, both effective radius and cloud optical depth can be expressed in terms of the above parameters (Liou, 1992):

$$r_{eff} = < r^3 > / < r^2 > \qquad (6)$$

$$\tau = \pi/4 \int Q_{ext}(\lambda,D) \, D^2 \, n(D) \, dD \, \Delta z \qquad (7)$$

These quantities, along with other parameters, enter into the formulation of the radiative transfer model as explained below.

3.2 VIS model

For the visible part of the spectra, we based our radiative model using the interaction principle and the doubling and adding method applied within a homogeneous atmosphere (e.g. van de Hulst, 1980). Due to the complexity of the model, the results are stored in terms of the reflectance function in terms of effective radius, cloud optical depth, solar zenith angle, satellite zenith angle, azimuth angle for both ice and water clouds at each of the visible wavelengths:

$$R(r_{eff},\tau,\mu,\mu_0,\Phi,p,\lambda) = \pi \, I(0,-\mu,\Phi) \, / \, \mu_0 F_0 \qquad (8)$$

where μ, μ_0, Φ describe the geometry of the scattering, p is the phase of the cloud (ice/water), and F_0 is the incoming solar flux. A simple three-layer model (atmosphere-cloud-surface) is then applied. Underlying surface albedo α is set to a standardized value depending on the surface type using the IGBP data set. Attenuation due to gases for the entire atmospheric column is also accounted for. Essential for the optimal estimation method is a good initial guess; therefore, a simple but efficient parameterization relating cloud optical depth to ch1 reflectance was used. In the same way, ch2 response, that combines both IR and VIS contribution, was parameterized in terms of the effective radius. Both these parameterizations are consistent with the technique introduced by Nakajima and King (1990).

3.3 IR model

For the thermal part of the spectra, using Planck's function to a homogeneous cloud, the radiative transfer equation is integrated from surface to top of the atmosphere:

$$I^{\uparrow}(0,\mu) = I_s(\mu) \exp(-\tau/\mu) + \int B(t) \exp(-t/\mu) \, dt/\mu \qquad (9)$$

Cloud top temperature is matched with the corresponding numerical model output; hence information about cloud top pressure and cloud top height can also be ascertained. Again, surface emission and clear atmosphere emission/absorption are accounted for. In addition, cloud effective emissivity is also estimated. The black-body assumption, corrected by an estimate of atmospheric transmission, is a good starting point for cloud top temperature in the optimal estimation iterative procedure.

3.4 Masking/Typing algorithm

In addition to the above quantitative characterization of the cloud filed, a qualitative approach is also

desirable. We refer here to the CLAVR-x cloud classification procedure of masking and typing (Heidinger, 2004). This technique checks a multi-spectral signal against pre-computed thresholds and assigns a class classification to the pixel. We mention the reflectance and thermal tests, four-minus-five test, spatial uniformity tests, and several restoral tests. However, since the expected range of multi-spectral response was determined within some restrictive environment conditions, occasionally the method can misinterpret a scene. This is more problematic over land regions and near the terminator, where changing terrain features and shadow effects are not yet well represented by models. In order to minimize such possible errors, the fixed thresholds limits must be replaced with parameterized ones. This is not an easy task, due to the complexity of the problem. A useful approach is to check the qualitative results against the quantitative output and make necessary corrections. One such example is presented further below, where the initial assignment was for a liquid cloud, but upon the non-convergence of the retrieval, the type was changed to cirrus.

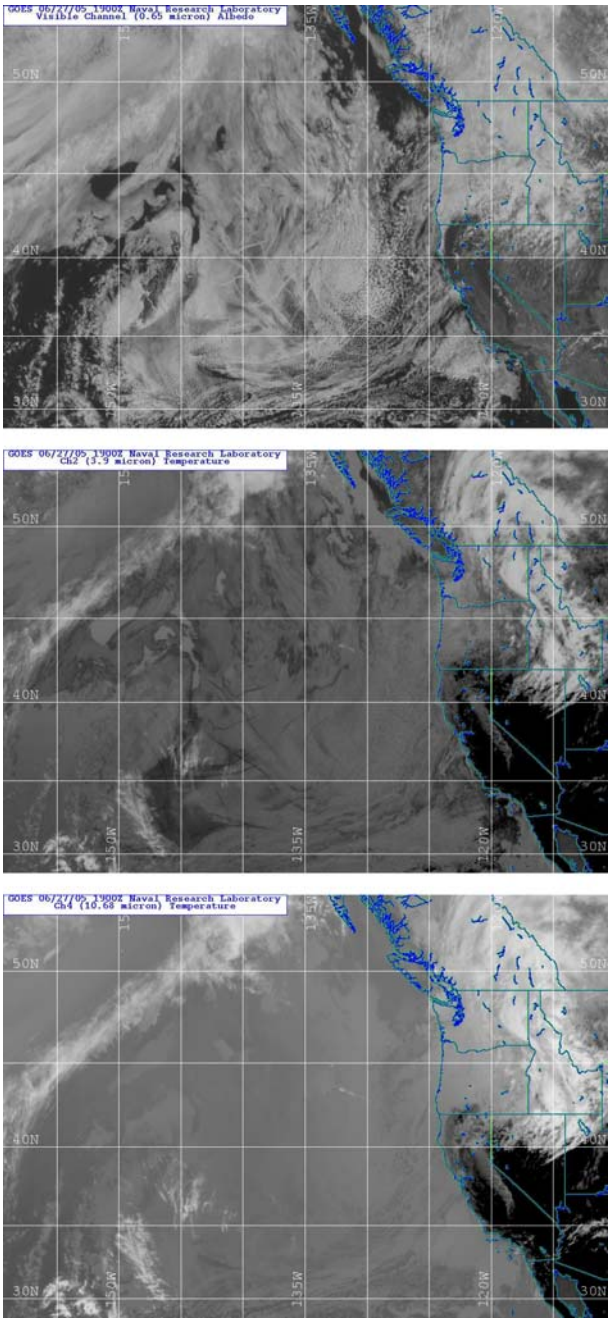

Figure 1. GOES-10: ch1, ch2, and ch4.

4. APPLICATION TO GOES DATA

4.1 27 June 2005, 1900Z daytime case study

Results from the application of the retrieval technique to measured data is applied to data from GOES-10 imager received on 27 June 2005, 1900Z, as an example of a daytime retrieval. The reader is encouraged to visit our NRL website at www.nrlmry.navy.mil/archdat/cloud_props/, where the technique is applied to both GOES-10 and GOES-12.

Figure 1 shows the input fields: ch1 VIS reflectance, ch2 NIR equivalent reflectance (reflected plus emitted), and ch4 IR temperature. The images, which depict an area of the eastern part of Pacific and western part of US, show a wide range of cloud types such as an extensive marine stratus layer, convective clouds associated with a frontal zone, and cirrus clouds, with clear sky regions. Also identifiable in both ch1 and ch2 images are ship tracks, referred to again later on.

Figure 2 shows the cloud classification according to the above mask/type algorithm. The masking classes are: clear, mix/clear, mix/cloudy, cloudy, and uniform cloudy. The typing classes are: clear, partly clear, liquid, super-cooled, glaciated, cirrus, overlap, and unclassifiable. A visual comparison with Figure 1, demonstrates the general performance of the classification algorithm, despite the different resolution of the channels used. Stratiform clouds are well distinguished from partly cloudy regions, and the vertical cloud structure is also captured, with regions of cirrus and/or lower clouds. However, some of the clear sky areas are classified as partly cloudy, which is more pronounced for regions over land. This is to be expected since the assumed thresholds used for such a classification are inferred from an ensemble of idealized cases, that incorporates a large temporal scale and over a broad range of underlying surfaces, and thus not case specific.

According to the cloud type determined as above, the retrieval algorithm uses either water or ice look-up tables of reflectance and transmittance to match observed radiances. In the current setting, we only consider these two distinct cases, even for the overlap (high cirrus over low cloud) regions, where ice clouds are being assumed. Future work must address these simplifications by considering a pre-defined cloud vertical structure that accounts for multiple cloud layers within a possible mixed phase state. Although ambitious, numerical model data output makes this problem tractable.

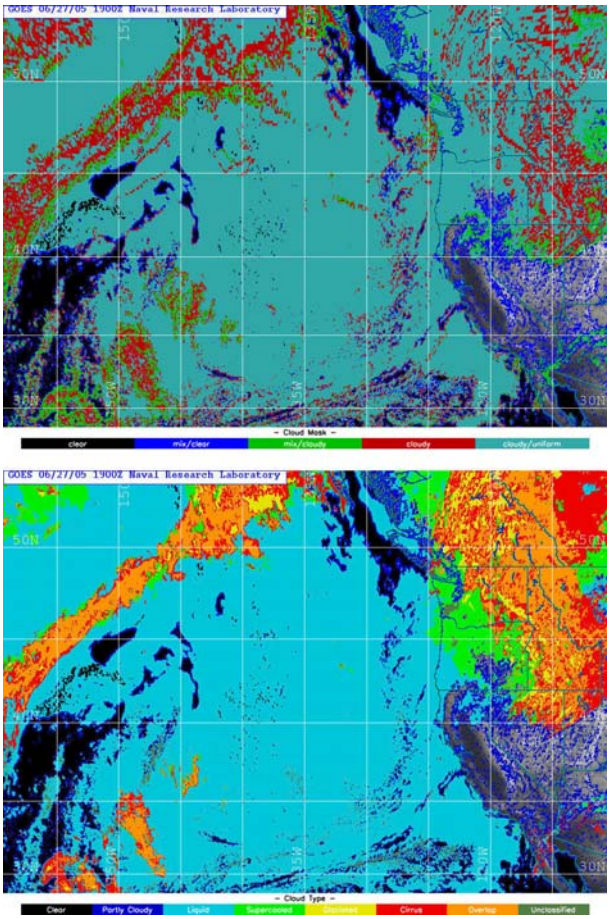

Figure 2. GOES-10: mask and type classification.

Figure 3 shows the retrieved quantities for the case considered: cloud optical depth, cloud top effective radius, and cloud top temperature. The cloud optical depth field shows a wide range of values, corresponding to a large variety of cloud types and structures. Sensitive to reflected solar radiation, this parameter gives a measure of the penetration depth, dependent to the cloud type and underlying surface. Overlapped clouds, associated with deep cloud layers, exhibit large values for tau, while thin cirrus clouds show the smallest values, due to their relatively high transparency. In particular, broken cloud fields show a higher optical depth at their centers compared to borders. Although not present in this example, cloud three-dimensional structure affects the retrieved values, especially at low solar angles.

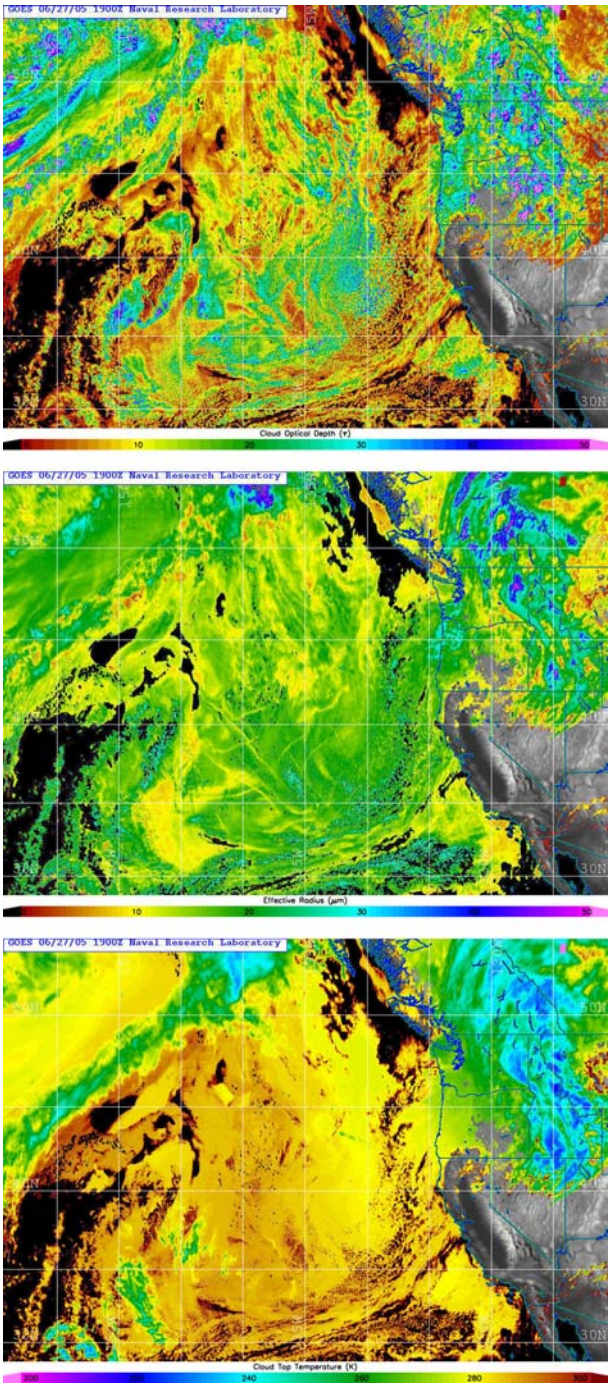

Figure 3: GOES-10 retrieved quantities: τ, r_{eff}, T_c.

Compared to τ, the effective radius shows only a reduced variability over the cloud field, with typical values of around 10 microns for low stratus (and fog), 20 microns for higher water clouds and above 30 microns for ice clouds. As previously noted, the ship tracks are clearly identifiable from the surroundings, by lower values of the effective radius due to increased CCN concentrations (Coakley et al., 1987) from ship effluents.

Finally, the retrieved cloud top temperature mimics that directly measured by the IR radiometer for optically thick clouds. Its determination is mostly due to information in this spectral region, although for thin clouds the optical depth and underlying surface temperature play an important role.

The quality of the retrieval - at pixel level - is demonstrated in Figure 4, where a false-color representation of the cost function (1) is presented. Its intent is to provide a quick and objective check of the retrieval and identify problem regions. One color is assigned to each of the channels and a brightness scale designates the level of error (in a linear representation). For ch1 and ch2, each color level represents a 1 % increment of albedo error, whereas a 0.5 K increment of temperature error is adopted for ch4. From the figure we note that overall, the retrievals errors are less than the above thresholds of errors, and only at the cloud boundaries - due to differences in pixel sizes for the channels used, the retrieval fails systematically. The upcoming NPOESS system, by adopting a uniform resolution throughout the measured spectra, addresses this issue.

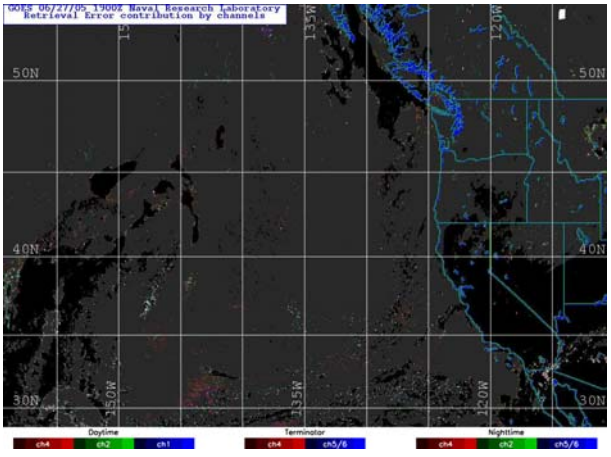

Figure 4: GOES-10 Retrieval errors.

Finally, Figure 5 shows derived quantities: cloud effective emission, cloud top height, and cloud liquid/ice water path. From the figure, we notice that in general, clouds behave as black-bodies with emissivities larger than 0.95. Occasionally, these values drop to 0.5 for thin and broken clouds for reasons explained above.

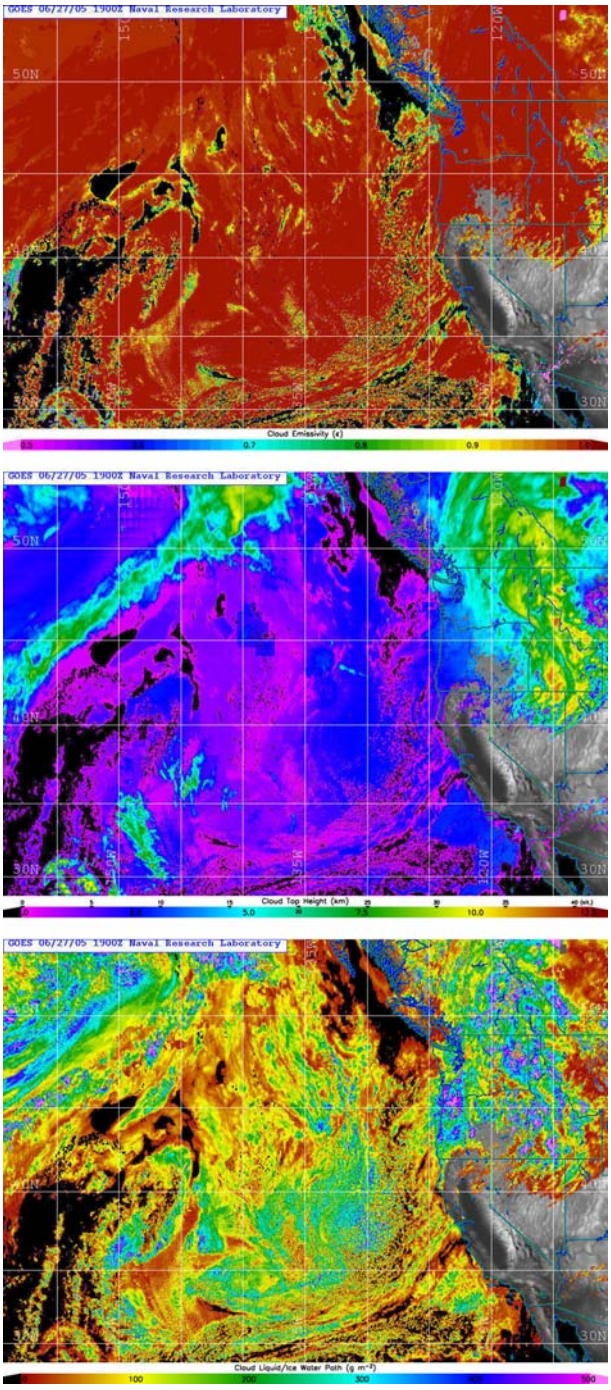

Figure 5: GOES-10 derived quantities: cloud emissivity, CTH and LWP/IWP.

Cloud top height, derived by matching the cloud top temperature to a numerical model temperature profile, provides a useful classification for the cloud field. However, due to inherent model errors (both spatial and

temporal), this parameter is subject to misrepresentation. In particular, for cases when persistent temperature inversions are present, lower clouds may be assigned to higher altitudes. In contrast, in the case of deep convective clouds, the model tropopause may be much lower than the real one, thus a lower than real cloud altitude is calculated. Therefore, for these particular cases a decision rule must be employed. This implies either an assignment to the inversion level or respectively a correction of the model tropopause to an equivalent one based on moist adiabatic lapse rate.

Cloud liquid or ice water path can also be evaluated. In the case of ice crystals, both density and non-spherical effects should be accounted for (Heymsfield et al., 2004). Presently, such a parameterization is not yet implemented, thus the values of this parameter are only crude estimates. An integrated quantity, LWP/IWP is closely related to the cloud optical depth.

5. SUMMARY AND CONCLUSIONS

A method for retrieving key cloud parameters using passive sensors is presented. The multi-spectral method introduced here targets the complex nature of clouds, as their multi- temporal and spatial scale structure can only be captured by satellite-borne instruments. The retrieval of cloud optical, microphysical, and thermodynamical properties follows a scheme that is framed around the optimal estimation method. Data from GOES-10 imager is used to demonstrate the method. In addition to cloud optical depth, cloud top effective radius, and cloud top temperature, fields of cloud effective emissivity, cloud top height, and LWP/IWP can also be derived. The radiative and microphysical model does not yet capture the entire 3D cloud effects. Future work, based on both observational studies (like the upcoming CloudSat and CALIPSO missions), as well as numerical model simulations should cast some light into this difficult problem.

Auxiliary to the retrieval method, cloud masking and typing provide valuable information about cloud phase, structure and extend. However, as above, this algorithm needs to be improved for the next generation of sensors (i.e. NPOESS observing system).

6. ACKNOWLEDGMENTS

We gratefully acknowledge the support of our research sponsor, the Office of Naval Research under program element PE-0602435N. The authors are thankful to Drs. A. Heidinger (NOAA) and M. Pavolonis (CIMSS) for providing the benchmark CLAVR-X retrieval software that was adapted here to the NRL automated processing system.

7. REFERENCES

Coakley, J.A., R.L. Bernstein and P.A. Durkee, 1987:
Effect of Ship-Stack Effluents on Cloud Reflectivity, *Science*, **237**, 1020-1022

Hartmann, D. L. and K. Larson, 2002:
An Important Constraint on the Tropical Cloud-Climate Feedback,
Geophys. Res. Lett., **29**, doi:10.1029/2002GL015835

Heidinger, A.K., 2004:
CLAVR-x Cloud Mask Algorithm Theoretical Basis Document,
NOAA/NESDIS/Office of Research and Applications, Washington, D.C.

Heidinger, A., 2003:
Rapid Daytime Estimation of Cloud Properties over a Large Area from Radiance Distributions,
J. Atmos. Oceanic Technol., **20**, 1237-1250

Held, I. M. and B. J. Soden, 2000:
Water Vapor Feedback and Global Warming,
Annu. Rev. Energy Environ., **25**, 441-475

Heymsfield, A.J., A. Bansemer, C. Smith, C. Twohy, M.R. Poellot, 2004:
Effective Ice Particle Densities Derived from Aircraft Data,
J. Atmos. Sciences, **61**, 982-1003

van de Hulst, H.C., 1980:
Multiple Light Scattering,
Academic Press, New York 1980

Jazwinsky, A.H., 1970:
Stochastic Processes and Filtering Theory,
Academic Press, 376 pp.

Liou, K.N., 1992:
Radiation and Cloud Processes in the Atmosphere,
Oxford University Press, 487 pp.

Liou, K. N., 1986:
Influence of Cirrus Clouds on Weather and Climate Processes: A Global Perspective,
Mon. Wea. Rev., **114**, 1167-1199

Miller, S.D., G.L. Stephens, C.K. Drummond, A.K. Heidinger and P.T. Partain, 2000:
A Multisensor Diagnostic Satellite Cloud Property Retrieval Scheme,
J. Geophys. Res., **105**, 19,955-19,971

Mitrescu, C., J.M. Haynes, G.L. Stephens, S.D. Miller, G.M. Heymsfield and M.J. McGill, 2005:
Cirrus Cloud Optical, Microphysical and Radiative Properties Observed During CRYSTAL-FACE Experiment: A Lidar-Radar Retrieval System,
J. Geophys. Res., **110**, doi:10.1029/2004JD005605

Nakajima, T. and M.D. King, 1990:
Determination of the Optical Thickness and Effective Particle Radius of Clouds from Reflected Solar Radiation Measurements. Part I: Theory,
J. Atmos. Sci., **47**, 1878-1893

Ramanathan, V. and W. D. Collins, 1991:
Thermodynamic Regulation of the Ocean Warming by Cirrus Clouds Deduced from Observations of the 1987 El Nino,
Nature, **351**, 27-32.